

LETTER • **OPEN ACCESS**

Radiatively tamed divertor thermal loading in resonant magnetic perturbation (RMP)-driven, ELM-crash-suppressed plasmas

To cite this article: Yongkyoon In *et al* 2024 *Nucl. Fusion* **64** 064001





View the [article online](#) for updates and enhancements.

You may also like

- [Integrated RMP-based ELM-crash-control process for plasma performance enhancement during ELM crash suppression in KSTAR](#)
Minwoo Kim, G. Shin, J. Lee et al.
- [Exploration of RMP ELM control on ITER-similar shape \(ISS\) in KSTAR](#)
Sang-hee Hahn, Y. In, N.W. Eidietis et al.
- [Preemptive RMP-driven ELM crash suppression automated by a real-time machine-learning classifier in KSTAR](#)
Giwook Shin, H. Han, M. Kim et al.

Letter

Radiatively tamed divertor thermal loading in resonant magnetic perturbation (RMP)-driven, ELM-crash-suppressed plasmas

Yongkyoon In^{1,*} , H.H. Lee², K. Kim² , A. Loarte³ , I.H. Choi¹, J.Y. Heo¹, Y.S. Han⁴, Wonho Choe⁴ , J. Hwang⁴ and H. Shin⁴

¹ Ulsan National Institute of Science and Technology, Ulsan, Korea, Republic Of

² Korea Institute of Fusion Energy, Daejeon, Korea, Republic Of

³ ITER Organization, Route de Vinon-sur-Verdon, CS 90 046, 13067 St. Paul Lez Durance Cedex, France

⁴ Korea Advanced Institute of Science and Technology, Daejeon, Korea, Republic Of

E-mail: inyongkyoon@unist.ac.kr

Received 10 December 2023, revised 21 March 2024

Accepted for publication 12 April 2024

Published 23 April 2024



CrossMark

Abstract

Edge-localized-modes (ELMs) suppression by non-axisymmetric resonant-magnetic-perturbation (RMP) provides the way to reach high performance fusion plasmas without a threatening level of transient heat fluxes to the walls of fusion devices. The application of RMP, however, strongly modifies the heat flux pattern onto in-vessel components in contact with the plasma (especially the divertor) leading to local ‘hot spots’. Radiative dissipation by partially ionized species (impurities and deuterium) lowers the heat flux peaks on the walls but has been poorly compatible with such RMP-driven, ELM-crash-suppression. Here, we show how KSTAR has radiatively tamed divertor thermal loading down to more than a factor of 7 in the off-separatrix region without losing ELM-crash-suppression using ITER-like, three-row, RMP configurations, demonstrating its sustainment even in a partially detached plasma in the outer strike point, as required for ITER.

Keywords: edge-localized-modes (ELM), resonant magnetic perturbation (RMP), ELM-crash-suppression, divertor thermal loading

(Some figures may appear in colour only in the online journal)

* Author to whom any correspondence should be addressed.



Original content from this work may be used under the terms of the [Creative Commons Attribution 4.0 licence](https://creativecommons.org/licenses/by/4.0/). Any further distribution of this work must maintain attribution to the author(s) and the title of the work, journal citation and DOI.

1. Introduction

The demonstration of thermonuclear fusion as an energy source using magnetically confined plasmas is the foremost goal in ITER, where high pressure ‘burning’ plasmas should be not only established but also sustained to exhibit power extraction capability [1, 2]. Considering that ITER high fusion gain (Q) scenarios are based on high confinement mode (H-mode) plasmas, the occurrence of edge-localized modes (ELMs) in H-mode plasmas [3] is very likely to pose a major integration issue that needs to be resolved in ITER operation scenarios. Specifically, the bursty release of particle and heat fluxes associated with ELMs can significantly erode plasma facing components (PFCs: main wall and divertor) reducing their operational lifetime. ELMs can also degrade the performance of confined fusion plasmas due to the accumulated impurity influxes they cause [4]. However, thanks to the remarkable progress in both theory [5, 6] and experiments [7–12] in recent years, such ELMs are expected to be fully suppressed in ITER, not just their severity reduced (i.e. ELM-mitigation), using the application of non-axisymmetric resonant magnetic perturbation (RMP). Despite tremendous progress in ELM-crash-mitigation studies, a generalized model does not exist to determine the requirements for ELM-crash-mitigation with RMPs in ITER yet. It is for instance unclear whether small ELM crashes will actually decrease the heat flux in ITER (e.g. [13]) and this drives the need for full ELM-crash-suppression in ITER. In this regard, it is essential that high performance fusion plasma operation with such RMP-driven, ELM-crash-suppression maintains the divertor heat fluxes under 10 MW m^{-2} in stationary conditions (ITER design limit). Experiments in the present tokamaks, as reported in KSTAR [14, 15] or EAST [16], show that the peak divertor heat flux of RMP-driven, ELM-crash-suppressed H-modes is typically higher (by more than a factor of 2–3) than a steady level of heat flux between ELMs in ELMy H-mode conditions (without RMP). This is due in part to the increased stationary heat flux associated with the absence of ELMs but, most importantly, attributable to the changes in edge plasma and heat transport dominantly from the confined plasma to the PFCs due to the three-dimensional fields created by the RMP.

In principle, a relatively straightforward solution to the heat flux exhaust problem in RMP-driven, ELM-crash-suppression is to increase the level of edge electromagnetic radiation by impurity seeding together with fuel gas puffing. In this way the level of radiation loss is enhanced (proportional to $n_e^2 Z_{\text{eff}}$) near the region of contact between the plasma and the wall in the divertor region (n_e refers to the plasma density and Z_{eff} is an effective atomic number characterizing the level of impurity ionization in plasmas). This scheme is routinely used to achieve the so-called radiative/detached divertor conditions with low divertor heat fluxes while maintaining high core confinement in present ELMy H-mode experiments without RMP, as has been extensively studied (e.g. AUG [17]). Unfortunately, when applied with RMP, such impurity/gas

fueled plasmas often lead to a loss of ELM-crash-suppression with a small reduction of the divertor heat flux with respect to the otherwise similar ELM-crash-suppressed conditions (typically less than a factor of 2) as found in KSTAR [15], and EAST [16]. Larger reductions, while sustaining RMP-driven, ELM-crash suppression, have been obtained in DIII-D and KSTAR [18, 19] but not through the increase of radiation in the divertor region but in the confined plasma. ITER is expected to operate with a partially detached high density divertor plasma so as to provide acceptable divertor power load handling [20], while maintaining a low core radiation to sustain the high confinement plasmas required for high fusion gain operation. Therefore, the compatibility of radiative divertor conditions with strongly reduced heat flux to the divertor with RMP-driven, ELM-crash-suppression remains an open issue for ITER. Of particular complexity and importance for ITER is the issue of achieving radiative divertor conditions and heat flux reduction in the 3D divertor structures away from the separatrix, which are created by the application of RMP. This was identified initially in experiments at EAST [21], understood to be directly linked to the 3D edge magnetic field geometry [22], and confirmed experimentally at EAST [16], where the off-separatrix heat flux could only be reduced by a factor of less than 1.5 through the increase of divertor density and impurity radiation before ELM-crash-suppression was lost. ITER-specific modeling has been in good progress to address both RMP ELM control and divertor thermal loading (e.g. JOREK) [23].

In this letter, we demonstrate, for the first time, a reduction of both the near-separatrix and off-separatrix heat flux in KSTAR significantly, while maintaining RMP-driven, ELM-crash-suppression and demonstrating its sustainment in a partially detached plasma near the outer strike point (OSP). This accomplishment is noticeably attributable to the following three major factors; (i) the optimal 3D magnetic field topology by applying currents in coils situated above/below and at the outer midplane, (ii) the use of N_2 impurity seeding to increase divertor radiated power levels and (iii) the use of ‘diffusive’ D_2 gas fueling to increase the edge/divertor plasma density. We note that KSTAR has a rather unique capability to optimize the applied 3D magnetic perturbations through its ITER-like configuration having three rows of in-vessel ELM control coils and, as we show in this letter, this is key to achieve the lowest divertor heat fluxes by enhanced divertor radiation while maintaining ELM-crash-suppression.

2. Experimental setup for divertor thermal loading under RMP-driven, ELM-crash-suppression

The layout of the ELM control coils, gas feed lines, divertor Langmuir probes, and diagnostics used in this study in the KSTAR tokamak, as well as the structural views of KSTAR and ITER in-vessel ELM coils, is shown in figure 1. While the equilibrium separatrix is delineated in D shape in grey in figure 1(a), the OSP on the divertor surface is referenced

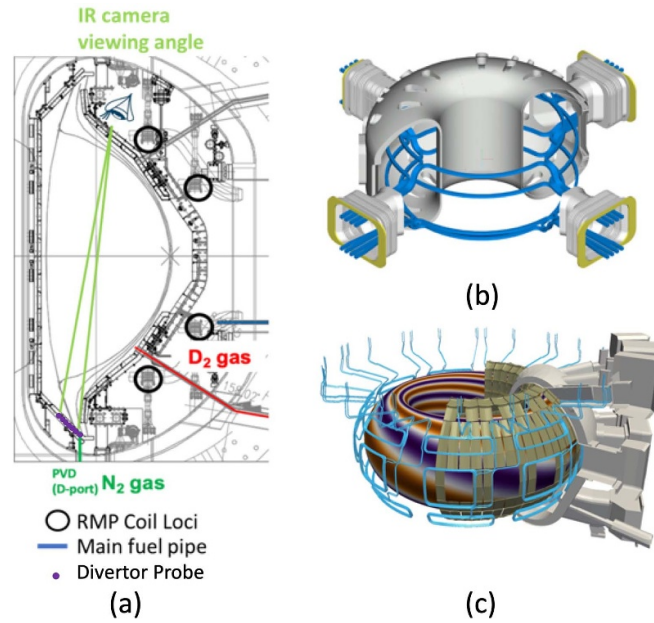


Figure 1. (a) Layout of the KSTAR tokamak highlighting the positions of the three rows of in-vessel ELM control coils (RMP coils Loci), the fueling lines used for diffusive plasma fueling (red) and impurity seeding (dark green) and the viewing geometry (light green) of the infrared camera system used to diagnose heat fluxes to the divertor target (structure at the bottom of the figure), along with divertor probes (magenta). (b) In-vessel Control Coils (IVCC) for RMP in KSTAR, and (c) In-vessel ELM control coils in ITER. Note that both KSTAR and ITER are similarly capable of providing a non-axisymmetric magnetic field using 3-rows.

to differentiate the near-separatrix (close to OSP) from off-separatrix (away from OSP) under RMP respectively.

In an initial set of experiments, a systematic study of the effect of the $n = 1$ 3D fields applied with the 3-rows of ELM control coils in comparison to the 2-rows, which are commonly available in other tokamaks, was carried out in KSTAR, as shown in figure 2. Here, n refers to the toroidal mode number, while $n = 1$ is the longest wavelength, non-axisymmetric field that typically allows ELM-crash-suppression to be achieved without triggering global MHD instabilities in the plasma discharge in fusion devices with a low level of intrinsic error fields [24]. This lower single null discharge had a toroidal magnetic field (B_T) of 1.8 T with plasma current (I_p) of 0.5 MA, dominantly heated by neutral beam injection (P_{NBI}) of 3.1 MW, along with a safety factor (q_{95}) of ~ 5 . As shown in figure 2(f), a gradual increase of static (for 0.5 s) and rotating (for 1 s at 1 Hz) RMP current waveform in three different levels is configured to not only measure the threshold of RMP ELM-crash-suppression, but also diagnose the striated divertor thermal loading via a single IR camera whose view is narrowly fixed to a finite toroidal segment. It should be noted that the level of current that needs to be applied in the rows of coils to achieve ELM-crash-suppression depends on the number of rows used with 2-rows requiring a larger coil current level than when using 3-rows. This is quite consistent with a perturbed ideal MHD calculation in which the required 3D magnetic field strengths for ELM-crash-suppression remains the same; i.e. the externally applied magnetic field with the two different configurations and two current levels would be equivalently shielded out by the same induced currents inside plasma in the ideal MHD picture [6]. Hence, the use of 3-rows allows

the achievement of ELM-crash-suppression at a lower level of RMP current than that of 2-rows. The former is accompanied by lower divertor heat fluxes both near the separatrix and off-separatrix than the latter. As can be seen in this figure and in more detail in the top row of figure 3, the achievement of ELM-crash-suppression increases the total divertor heat flux in both 2-row and 3-row cases, but the increase is smaller with 3-rows than with 2-rows.

This result is, to some extent, consistent with a wider (by 10%–40%, in the toroidally averaged sense) divertor heat flux footprint for ELM-crash-suppressed conditions for 3-rows compared to 2-rows RMP, as had been previously identified in systematic experiments in KSTAR [14, 15, 25]. Despite this robust experimental evidence, the differences of the poloidally varying 3D magnetic field structure between 2 and 3 rows and their impact on edge transport are not fully understood yet. It is important to note that the peak values of the divertor heat flux are similar near the separatrix and in the off-separatrix structures when RMPs are applied, as shown in the top row of figure 3. To measure the full toroidal distribution of the divertor heat fluxes, the 3D magnetic field perturbation applied with 2 and 3 rows is rotated rigidly in the toroidal direction for 1 s at 1 Hz, while maintaining ELM-crash-suppression. This allows us to diagnose the divertor heat fluxes in a full coverage of the toroidal variation with one infrared camera located at a single toroidal location. Such a novel operation is possible in KSTAR, primarily due to its extremely low level of intrinsic $n = 1$ non-axisymmetric field [24], which could have otherwise spoiled the full toroidal scan.

To address the radiative thermal loading impact on such RMP-driven, ELM-crash-suppressed discharges, N_2 seeding

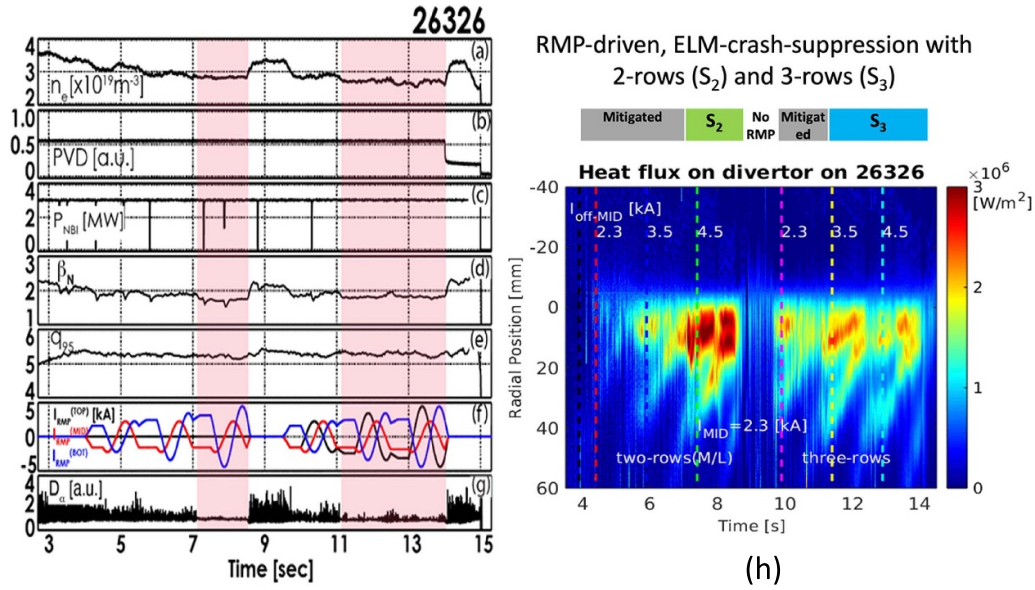


Figure 2. RMP-driven, ELM-crash suppression with 2-rows and 3-rows (shaded bands, ELM mitigation for non-shaded times) in KSTAR. Shown are the time traces of (a) line-averaged plasma density n_e , (b) divertor deuterium gas (0.6 V, equivalent to the rate of 1.3×10^{20} D_2 particles s^{-1}), (c) NBI heating power P_{NBI} , (d) normalized β , β_N , (e) safety factor, q_{95} , (f) RMP coil current per turn at top (black), middle (red), and bottom (blue) rows, (g) photodiode signal at lowest energy spectral line of deuterium Balmer series D_α (652 nm) respectively, and (h) Measured heat flux on the outer KSTAR divertor target (near the bottom of figure 1(a)) for ELM-mitigated and ELM-suppressed conditions, whose time evolution at each level of RMP current (static for 0.5 s, and rotating for 1 s at 1 Hz) shows a toroidally distributed pattern on the divertor.

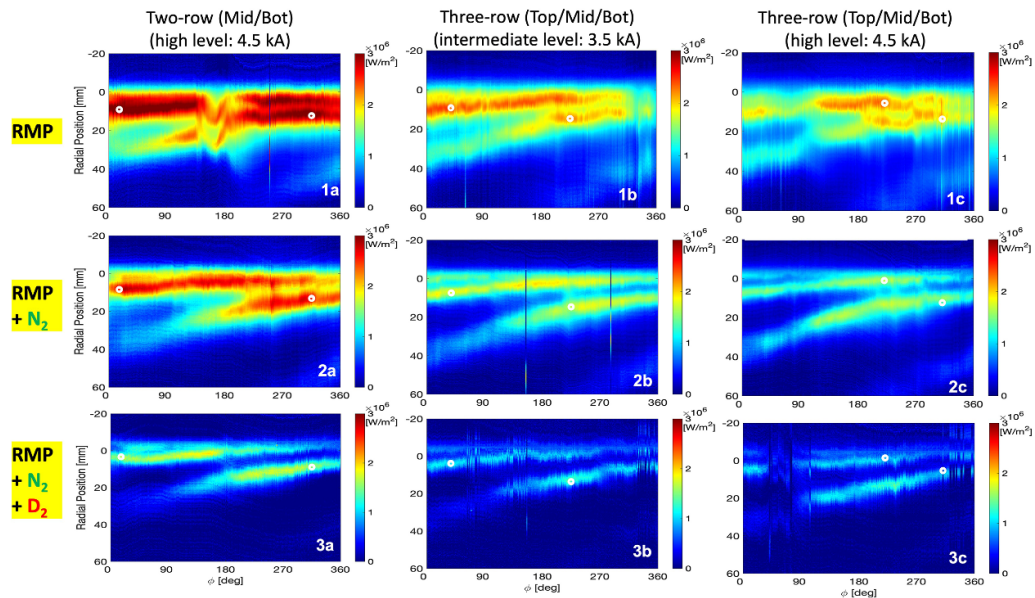


Figure 3. Toroidal distribution of divertor heat fluxes for 2-row and 3-row (with two levels of RMP current at 3.5 kA and 4.5 kA) ELM-crash-suppressed H-modes in KSTAR. Shown are the contours of power flux on divertor only with RMP in the top row (1a)–(1c), compared with those of RMP plus N_2 divertor seeding in the mid-row (2a)–(2c), and with the counterparts of RMP plus N_2 divertor seeding and diffusive off-divertor D_2 fueling in the bottom-row (3a)–(3c). The circles in the top row represent the loci of the peak heat fluxes in the near- and off-separatrix areas respectively, whose magnitude has been decreased by divertor radiation. These are used for quantitative comparisons of the heat flux reduction achieved when nitrogen and diffusive deuterium are additionally injected, as marked in the middle and bottom rows respectively. Note that N_2 + diffusive D_2 is the most effective in reducing heat fluxes for 2-row and 3-row without losing the RMP-driven, ELM-crash-suppression, demonstrating its sustained compatibility with a partially detached plasma in (3c), as discussed in the paper.

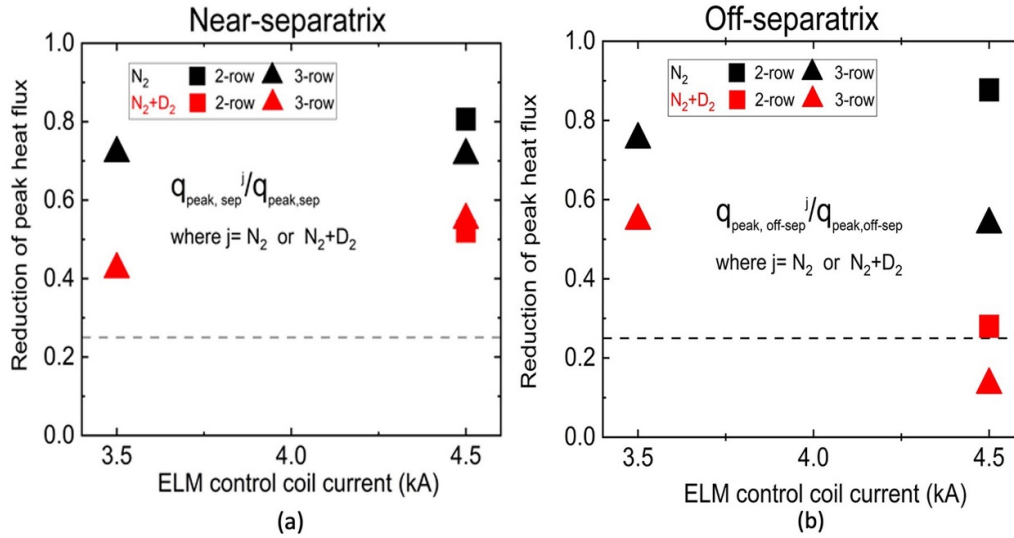


Figure 4. Comparison of the heat flux reduction associated with the divertor thermal loading control during RMP-driven, ELM-crash-suppression. (a) Ratio of the power flux near the separatrix ($0 < R < 12$ mm) without gas control at the toroidal location in which it is maximum ($q_{\text{peak, sep}}$) to that ($q_{\text{peak, sep}}^{\text{N}_2}$) with N₂ divertor seeding (black), and to that ($q_{\text{peak, sep}}^{\text{N}_2 + \text{D}_2}$) with diffusive D₂ off-divertor fueling plus N₂ divertor seeding (red) for 2-row (square) q_{peak} and 3-row (triangle) ELM suppressed H-modes in KSTAR. (b) Ratio of the power flux ($q_{\text{peak, off-sep}}$) away from the separatrix ($R > 12$ mm) and the counterparts (i.e. ($q_{\text{peak, off-sep}}^{\text{N}_2}$ and $q_{\text{peak, off-sep}}^{\text{N}_2 + \text{D}_2}$) under the same corresponding conditions. Each circle in figure 3 denotes the toroidal angle and radial position used for the comparisons evaluated here. According to the same definition, a factor of 4 is horizontally delineated, as required for ITER operation scenarios [24].

and diffusive D₂ + N₂ injection were added from $t = 3$ s in a steady level (N₂: $4.1 \times 10^{20} \text{ s}^{-1}$ and diffusive D₂: $5.6 \times 10^{19} \text{ s}^{-1}$), while maintaining the ELM-crash-suppressed H-mode state and a strong reduction of divertor heat fluxes. All the core plasma parameters in these discharges remain essentially the same, despite the various changes of edge and SOL conditions, showing a similar line-averaged plasma density of $n_e \sim 3 \times 10^{19} \text{ m}^{-3}$ (commensurate with $\sim 40\%$ of Greenwald density limit) at $q_{95} \sim 5$. The experimental results are shown in the middle row of figure 3 (for N₂), and in the bottom row of figure 3 (for D₂ + N₂) respectively. It is to be noted that the use of 3-row RMPs at high level (4.5 kA) has lowered the divertor thermal loading than at intermediate level (3.5 kA), which has eventually led to more than a factor of 4 reduction in the off-separatrix region without driving a $n = 1$ mode-locking.

3. Radiatively controlled divertor thermal loading and partial detachment near outer strike point

3.1. Divertor heat flux reduction associated with radiative SOL control

For a quantitative analysis in near- and off-separatrix heat flux reduction in detail, we have selected only the fully ELM-crash-suppressed periods at both 2 and 3 rows of RMPs, where the off-midplane coil current amplitude per turn is either 3.5 kA or 4.5 kA with fixed midplane coil current amplitude at 2.3 kA. While N₂ seeding has lowered the maximum divertor heat flux, the combination of diffusive D₂ and N₂ seeding has been most effective in both 2-row and 3-row RMPs. Of particular importance for ITER is to quantify this reduction of divertor heat fluxes at the toroidal location where they are highest,

both at the separatrix and off-separatrix. Specifically, for ITER $Q = 10$ plasmas without RMP, a reduction of a factor of, at least, 4 by radiative divertor operation is required to reduce the maximum heat flux under engineering design limits, from 2D modeling results which results in a scrape-off layer heat flux fall-off length (λ_q) of 3.4 mm [26]. It is to be noted that such λ_q estimate for ITER remains very uncertain. For example, an empirical scaling for ITER power-decay length guided by an heuristic drift model is extrapolated to be of the order of ~ 1 mm [27], while a theoretical prediction based on gyrokinetic simulations is projected up to 5.9 mm [28]. In a typical RMP experiment in KSTAR, a similar power-decay length of ~ 2 mm has been measured without RMPs [15], which is not affected by extrinsic gas inputs, while the divertor is attached [14, 15]. For RMPs with low gas input, a toroidally averaged power decay length remains similar to that of no RMP discharge (e.g. ~ 2 mm in KSTAR). In this regard, the influence of radiative thermal loading control should be quantified in terms of the heat flux reduction at the highest divertor heat flux locations, rather than other heat flux quantities such as time-averaged ones (e.g. [14, 15, 29]) since a local ‘hot spot’ determines the integrity of the in-vessel components. As shown in the top row of figure 3, it is commonly observed that the magnitude and toroidal phase of the near-separatrix peak ($q_{\text{peak, sep}}$) are different from those of the off-separatrix peak ($q_{\text{peak, off-sep}}$), so that the examination of ‘hot spots’ in both near-separatrix and secondary lobes should be performed independently without selecting the same toroidal angle for both. Thus, the loci of such heat flux peaks in the near- and off-separatrix with RMP only, as circled in the top row of figure 3, have been used as reference to quantify the thermal loading variations under radiative control. For that

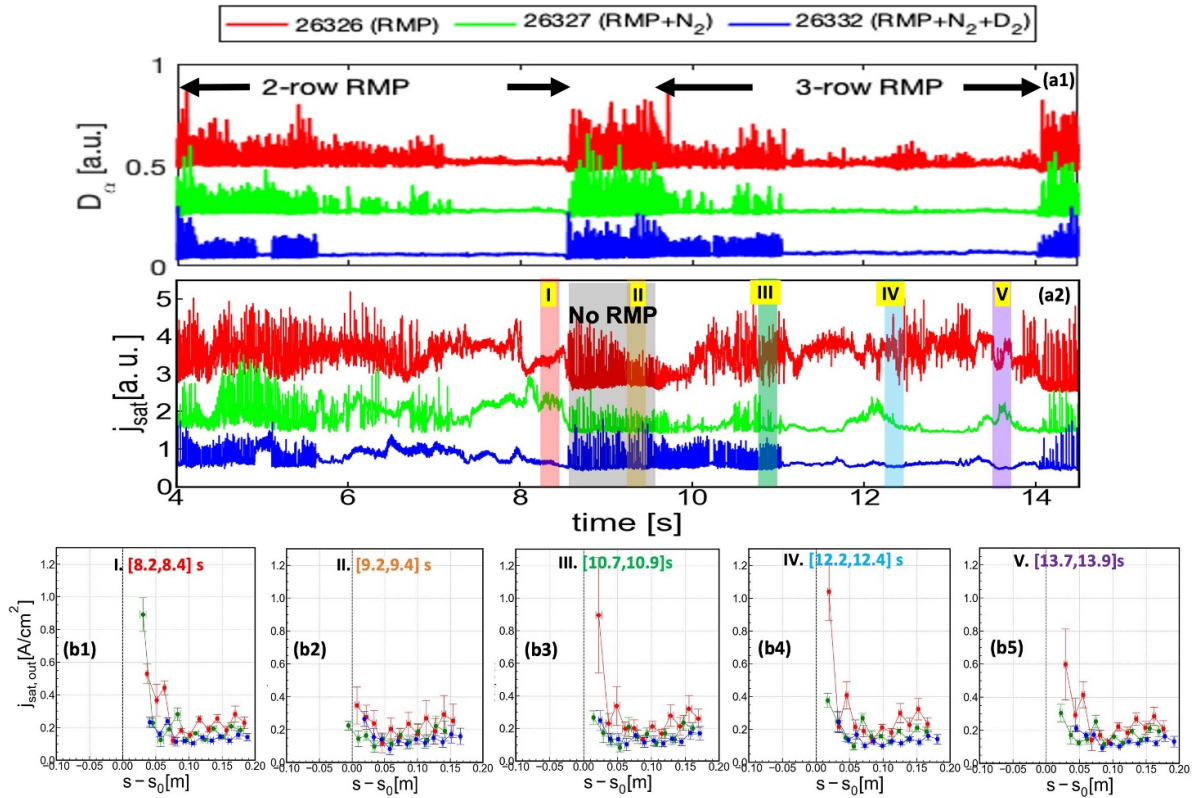


Figure 5. Time-evolutions of the photodiode signal of D_α in (a1) and ion saturation currents (j_{sat}) near the OSP in (a2), and the radial profiles of j_{sat} in each stage of the discharges in (b1)–(b5). Note that the discharge #26332 (blue) remained partially detached with 3-row RMP-driven, ELM-crash-suppression, as evidenced by the probe measurements in (b2)–(b5).

reason, the circles in the middle and bottom rows in figure 3 are not necessarily corresponding to the loci of the local peaks in angle. It is to be noted that any localized peak of the heat flux at the divertor with radiative gas control never reaches a higher value than without it in the top row of figure 3 (i.e. this is clear from the very small or negligible ‘hot spots’ in the middle and bottom rows of figure 3). Figure 4 shows a summary of such heat flux reductions achieved in the KSTAR experiments, when the gas control of N₂ and N₂ + D₂ is applied on top of RMPs. Specifically, each heat flux reduction at the near- and off-separatrix is defined as $(q_{peak, i}^j/q_{peak, i})$ with reference to the peak heat flux without gas control (i.e. $q_{peak, i}$), where i is the location of either ‘separatrix’ or ‘off-separatrix’, and j refers to the gas control of ‘N₂’ seeding or ‘N₂ + D₂’ injection respectively, as marked by the circles in figure 3. It is to be noted that a larger heat flux reduction occurs at the off-separatrix locations, which suggests a much more effective reduction of the thermal loading than in near-separatrix. In addition, the largest reduction of the heat fluxes under gas control has been achieved through increased divertor radiation, as shown in the combination of N₂ seeding and diffusive D₂ fueling, and the choice of RMP configuration (3-rows, rather than 2-rows) and strengths (i.e. coil current amplitudes).

3.2. Compatibility of RMP-driven, ELM-crash-suppression with partial detachment near the outer strike point

Figure 5 shows the time-evolutions of the photodiode signal of D_α and the time-average of 3 divertor Langmuir probes near the OSP, as well as the corresponding j_{sat} profiles of these discharges in various conditions for comparison. Due to the use of N₂ + diffusive D₂, detached divertor conditions are achieved for 26332 (blue) at 9 s when RMPs are not active showing very low j_{sat} near the separatrix. These low j_{sat} conditions are also found for the later times (i.e. time periods of IV and V in figure 5), in which both radiative gas control and 3-row RMP-driven, ELM-crash-suppression periods are maintained. For all the other combinations of 2-row and 3-rows with/without N₂, the ion flux increases substantially near the separatrix consistent with attached (or re-attached) conditions of the divertor. One of the noticeable observations is an easier access to RMP-driven, ELM-crash-suppression with N₂ and diffusive D₂ gas injection for 2-row RMP, though the j_{sat} was not clearly detached yet, as shown in the blue traces of figure 5(a1) and (a2).

Together with the decrease of divertor heat fluxes under gas control, the power radiated by the plasma increases. The region

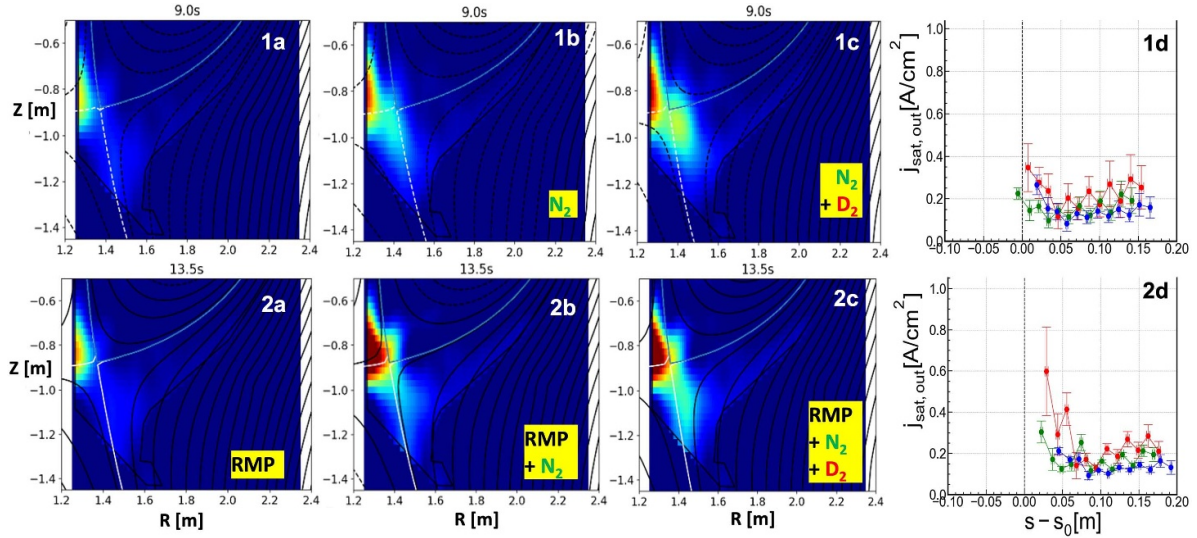


Figure 6. Measurements of plasma radiated power (P_{rad}) on calibrated foil bolometer and corresponding ion saturation currents on divertor Langmuir probes. Without RMP in the upper row, all the ion saturation currents in the OSP in (1d) remain low (nearly detached) similar to that in 1a (red), 1b (green) and 1c (blue) respectively, irrespective of P_{rad} increase. In comparison, with RMP in the lower row, when P_{rad} increases, the attached conditions (red and green in (2d)), corresponding to (2a) and (2b) become partially detached (blue in (2d)), corresponding to (2c), whose ion saturation currents are comparable to what was measured without RMP in 1d. It is to be noted that the increased radiation level, leading to the measured heat flux reduction on the divertor, remains confined to the divertor region as required in ITER high fusion performance operation.

with increased radiation remains in the divertor volume itself, as shown in figure 6. This is an important difference compared to similar studies including the prior observations in KSTAR [16, 18, 19], in which a significant proportion of the additional radiation created by impurities comes from the confined core plasma [18].

The KSTAR findings are of particular importance for the integration of ELM-crash-suppressed plasmas in view of high confinement plasmas and acceptable heat fluxes to the divertor for the following reasons: (a) the increased levels of radiation to reduce the divertor heat fluxes should not affect plasma confinement and thus fusion power production level in ITER; (b) a significant reduction of off-separatrix heat fluxes (roughly more than a factor of 4) remained the main outstanding issue regarding radiative divertor operation in RMP-driven, ELM-crash-suppressed H-mode in ITER since the off-separatrix heat flux levels could not be substantially reduced until now [16, 21, 22]; and (c) the use of ITER-like 3-row RMP configuration allows access to a larger level of heat flux reduction than that of 2 rows thus allowing a higher flexibility to meet the multiple requirements regarding plasma confinement, and transient and stationary heat flux control required to demonstrate fusion power production in ITER. We note that such flexible capability of 3-row RMP coil system has already been found essential to optimize a number of other integration issues in ITER scenarios with ELM-crash-suppressed conditions, such as for the reduction of fast particle losses [30].

4. Discussion

Regarding the extrapolation to ITER from the radiative divertor results in KSTAR with RMP-driven, ELM-crash-suppression, it is important to determine whether the radiative divertor conditions achieved in KSTAR correspond to a semi-detached divertor plasma state, as required for ITER plasmas to reach high radiative divertor conditions, as well as for a more preferable condition for good helium exhaust [31]. The imaging bolometer radiation measurements in figure 6 show that the radiation (dominated by nitrogen) extends all along the outer divertor region towards the divertor target, while the ELM-crash-suppressed state is sustained together with N_2 or $D_2 + N_2$ injection; this has been normally identified with attached divertor plasma conditions near the OSP in KSTAR. On the other hand, for normal ELMy H-mode (with no RMP) plasmas with $N_2 + D_2$ injection (e.g. near $t = 9$ s in figure 2 under similar setting), a noticeable increase of the radiation away from the divertor plasma was shown in figure 6(1a)–(1d), consistent with semi-detached divertor plasma conditions. Based on the ion saturation currents (j_{sat}) measured on divertor Langmuir probe [32], such detached plasma on 26332 at 9 s (blue in (1d) of figure 6) was found to have been sustained even during RMP-driven, ELM-crash-suppression periods, as ascertained in the blue trace of figure 6(2d). Although the OSP (vertical line) appears to have slightly shifted under rotating RMP due to magnetic reconstruction

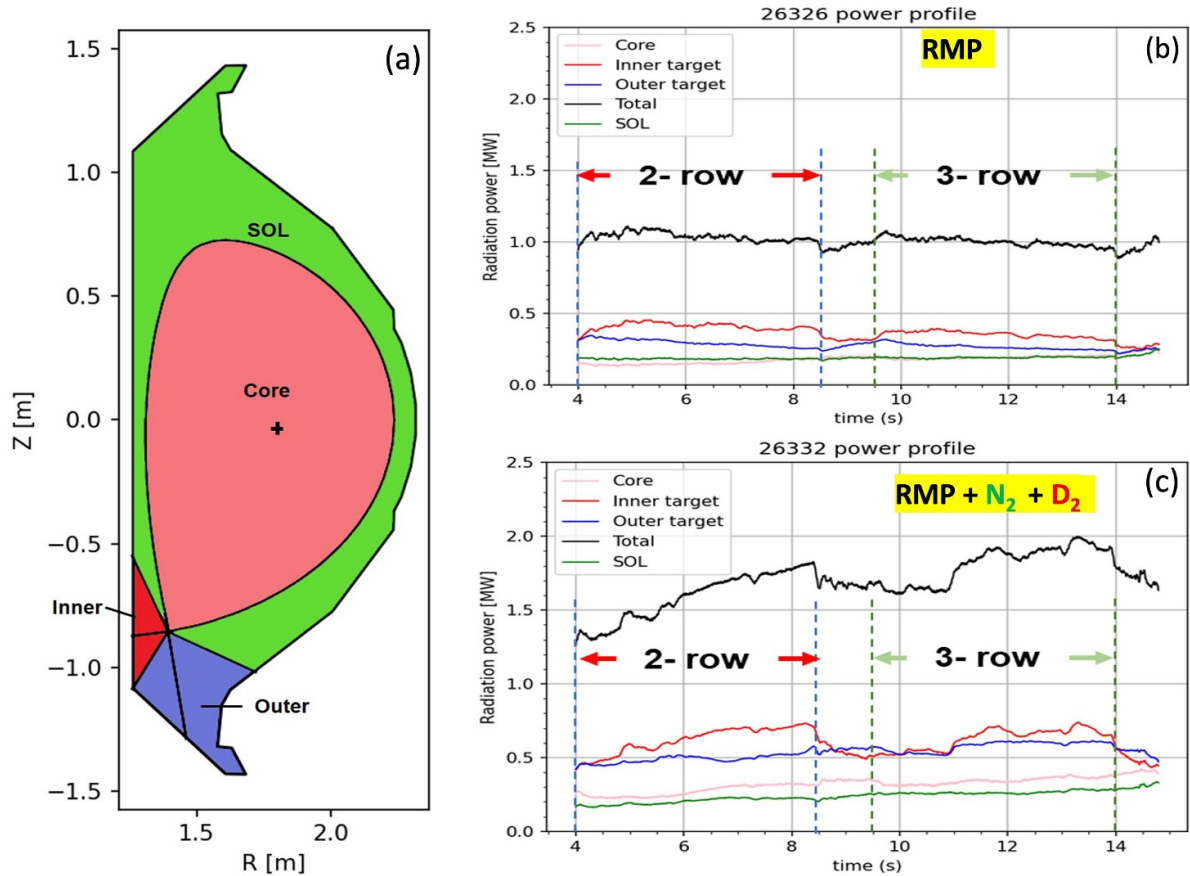


Figure 7. Time-evolution of radiative power (P_{rad}) based on visible bremsstrahlung tomography. Shown in (b) and (c) are the time traces of respective P_{rad} , corresponding to each region color-shaded in (a). In the vicinity of inner and outer strike points (red and blue respectively), the time-variations are also shown.

uncertainties, all the three fixed Langmuir probes remain in the vicinity of the OSP, as evidenced in the substantially elevated signal (red in the (2d) of figure 6) during attached condition.

To quantify the divertor thermal loading with respect to the time-varying radiative loss, the whole tomography analysis of visible bremsstrahlung has been done, as summarized in figure 7. Overall, the steady injections of N_2 and $\text{N}_2 + \text{D}_2$ have increased the total radiation power up to 70% (i.e. 0.7 MW, not shown here) and 90% (i.e. 0.9 MW) near $t = 13$ s respectively, while ITER-like three-row, RMPs remain successful in suppressing the ELM-crashes. To reach detachment without RMPs in the OSP, approximately 60% (i.e. 0.6 MW) radiation increase was required, as shown near $t = 8.5\text{--}9.5$ s in figure 7. As a result, the application of three-row RMP has elevated the radiative power loss due to the interaction of more particles and impurity gas in the SOL (attributable to RMP-induced, density pump-out and/or 3D field-driven SOL structure change) by approximately 0.3 MW. Here, the ELM-crash-suppression has been sustained without losing a partially detached condition near the OSP in KSTAR. It is to be noted that the power balance analysis shows a higher radiative

loss in the inner strike point than in the OSP, consistent with experimental observations as shown in figure 6. In terms of the applicability to ITER, we also note that, while the optimization strategy of 3D fields for ELM suppression with 3-rows for radiative divertor operation will be likely be applicable to ITER, the specific choice of N_2 impurity for KSTAR is not likely to be adopted in ITER. Rather, the optimum choice of impurity (or impurity mix) will be determined by the specific plasma conditions to be achieved at the divertor target both for near-separatrix and off-separatrix locations as already pointed out by studies in [33].

5. Conclusion

We have demonstrated for the first time in KSTAR that a radiative divertor regime with low heat fluxes throughout the toroidal and poloidal divertor target extents can be achieved with RMP, while maintaining an ELM-crash-suppressed H-mode and low level of core plasma radiation in a partially detached plasma near the OSP, as required for the integration of such scenario with high fusion gain operation

in ITER. While several issues remain to be understood in detail with a view to the physics-based extrapolation of these experimental results to ITER, we have shown that a significant reduction of off-separatrix heat fluxes in these conditions (a factor of more than 7 in figure 4) is possible in a partially detached plasma, unlike previous findings, through the simultaneous optimization of edge deuterium fueling, impurity seeding and the ITER-like 3D edge magnetic field applied to achieve the ELM-crash-suppressed state in KSTAR. The experimental results will help us validate various divertor transport modeling tools in ITER, such as EMC3-EIRENE under RMP ELM control [22, 33]. Taking into account the same physics actuators available in ITER, a similar strategy of RMP-driven, ELM-crash-suppression in combination of divertor thermal loading control is expected to support the accomplishment of the associated physics objectives required for fusion power demonstration in ITER.

Acknowledgments

This work was supported by the Korean Ministry of Science and ICT for the KSTAR project (KFE-EN2201-12), National and Research Fund (NRF-2019M1A7A1A03088443 and RS-2022-00155960), as well as through active collaboration with the ITER Organization. We acknowledge all the KSTAR Team members that have led the successful operations throughout the physics experiments.

ITER disclaimer

ITER is the Nuclear Facility INB No. 174. The views and opinions expressed herein do not necessarily reflect those of the ITER Organization

ORCID iDs

Yongkyoon In  <https://orcid.org/0000-0002-9219-1304>
 K. Kim  <https://orcid.org/0000-0002-6937-1761>
 A. Loarte  <https://orcid.org/0000-0001-9592-1117>
 Wonho Choe  <https://orcid.org/0000-0002-8952-8252>

References

- [1] Perkins F.W. *et al* 1999 *Nucl. Fusion* **39** 2137
- [2] Shimada M. *et al* 2007 *Nucl. Fusion* **47** S1
- [3] Zohm H. 1996 *Plasma Phys. Control. Fusion* **38** 105
- [4] Loarte A. *et al* 2014 *Nucl. Fusion* **54** 033007
- [5] Becoulet M. *et al* 2014 *Phys. Rev. Lett.* **113** 115001
- [6] Park J.-K. *et al* 2018 *Nat. Phys.* **14** 1223
- [7] Evans T.E. *et al* 2004 *Phys. Rev. Lett.* **92** 235003
- [8] Liang Y. *et al* 2007 *Phys. Rev. Lett.* **98** 265004
- [9] Suttrop W. *et al* 2011 *Phys. Rev. Lett.* **106** 225004
- [10] Jeon Y.M. *et al* 2012 *Phys. Rev. Lett.* **109** 035004
- [11] Kirk A. *et al* 2013 *Nucl. Fusion* **53** 043007
- [12] Sun Y. *et al* 2016 *Phys. Rev. Lett.* **117** 115001
- [13] Thomsen H. *et al* 2011 *Nucl. Fusion* **51** 123001
- [14] In Y. *et al* 2019 *Nucl. Fusion* **59** 056009
- [15] In Y., Loarte A., Lee H.H., Kim K., Jeon Y.M., Park J.K., Ahn J.-W., Park G.Y., Kim M. and Park H. 2019 *Nucl. Fusion* **59** 126045
- [16] Jia M.N. *et al* 2021 *Nucl. Fusion* **61** 106023
- [17] Kallenbach A. *et al* 2021 *Nucl. Fusion* **61** 016002
- [18] Orlov D.M., Moyer R.A., Bykov I.O., Evans T.E., Teklu A.M. and Lee J. 2018 Favorable impact of RMP ELM suppression on divertor heat fluxes at ITER-like conditions *Proc. 27th IAEA Fusion Energy Conf. (Ahmedabad, India, 22–27 October 2018)* p [EX/P6–17] (available at: <https://www.osti.gov/servlets/purl/1570889>)
- [19] Shin H., Hwang J., Han Y., Shin G., Lee H., Chai K.B. and Choe W. 2023 *Nucl. Fusion* **63** 044003
- [20] Kallenbach A. *et al* 2015 *Nucl. Fusion* **55** 053026
- [21] Li J. *et al* 2013 *Nat. Phys.* **9** 817
- [22] Frerichs H., Schmitz O., Bonnin X., Loarte A., Feng Y., Li L., Liu Y.Q. and Reiter D. 2020 *Phys. Rev. Lett.* **125** 155001
- [23] Becoulet M. *et al* 2022 *Nucl. Fusion* **62** 066022
- [24] In Y., Park J.K., Jeon Y.M., Kim J. and Okabayashi M. 2015 *Nucl. Fusion* **55** 043004
- [25] In Y. *et al* 2017 *Nucl. Fusion* **57** 116054
- [26] Pitts R. *et al* 2019 *Nucl. Mater. Energy* **20** 100696
- [27] Eich T., Sieglin B., Scarabosio A., Fundamenski W., Goldston R.J., Herrmann A. and Team A.U. 2011 *Phys. Rev. Lett.* **107** 215001
- [28] Chang C.S. *et al* 2017 *Nucl. Fusion* **57** 116023
- [29] In Y. *et al* 2022 *Nucl. Fusion* **62** 066014
- [30] Sanchis L. *et al* 2021 *Nucl. Fusion* **61** 046006
- [31] Loarte A. 2001 *Plasma Phys. Control. Fusion* **43** R183
- [32] Loarte A. *et al* 1998 *Nucl. Fusion* **38** 331
- [33] Frerichs H., Bonnin X., Feng Y., Li L., Liu Y.Q., Loarte A., Pitts R.A., Reiter D. and Schmitz O. 2021 *Nucl. Fusion* **61** 126027